SUPERCRITICAL, SUPERCOOLED: WATER AT LOW TEMPERATURES

Mikhail A. Anisimov
Institute for Physical Science & Technology and Department of Chemical & Biomolecular Engineering, University of Maryland, College Park, MD 20742, U.S.A.

Abstract

Liquid water is still a puzzle. Unlike ordinary substances, one can regard water near the triple point and in the supercooled region, on the one side, and water near the vapor-liquid critical point, on the other side, as "the same substance – two different liquids". Highly-compressible, low-dielectric-constant near-critical water is commonly used as a supercritical-fluid solvent. On the low-temperature side of the phase diagram, water is an almost incompressible, high-dielectric-constant solvent with some mysterious properties. In this region, some of the puzzles of liquid water can be explained by the virtual existence of the liquid-liquid critical point in metastable supercooled region. Therefore, supercooled liquid water can be regarded as a specific "supercritical fluid". In particular the concept of the Krichevskii parameter, which controls the behavior of supercritical fluid solutions near the solvent vapor-liquid critical point, can be generalized to supercooled water solutions. Fluctuations of entropy, diverging at the liquid-liquid critical point, may be associated with anomalous sensitivity ("susceptibility") of water structure to external perturbations and may also be responsible for mysterious behavior of some nonelectrolyte aqueous solutions. By stabilizing the fluctuations of water structure, through self-assembly of small organic molecules in aqueous solutions, one can create unusual nanoparticles and novel smart materials.

I. Introduction. Water: One Substance – Two Different Liquids

Unlike ordinary substances, one can regard water near the triple point and in the supercooled region, on the one side, and water near the vapor-liquid critical point, on the other side, as "the same substance – two different liquids". This can be illustrated by the behavior of the dielectric constant shown in Fig. 1. Highly-compressible, low-dielectric-constant near-critical water is commonly used as a supercritical-fluid solvent. On the low-temperature side of the phase diagram, water is an almost incompressible, high-dielectric-constant solvent with some mysterious properties. In this region, some of the puzzles of liquid water can be explained by the virtual existence of the liquid-liquid critical point in metastable supercooled region, as already suggested by the behavior of the isobaric heat capacity shown in Fig. 2

In 1971, Voronel [1] speculated that the liquid state of some substances might be envisioned as a state between two singularities: the gas-liquid critical point and the absolute stability limit of the liquid phase located below the triple-point temperature (see also ref. [2], p. 387). At that time, calorimetric measurements in water [3] indeed showed a noticeable increase of the isobaric heat capacity upon modest supercooling (~-8°C). However, the breakthrough in this field came with Angell et al.'s publication in 1973 [4] of accurate heat-capacity measurements of supercooled water emulsified in heptane, made using a procedure developed by Rasmussen and MacKenzie [5]. Reaching temperatures as low as -39°C at atmospheric pressure,

Angell and co-workers [6,7] observed a sharp increase in the isobaric heat

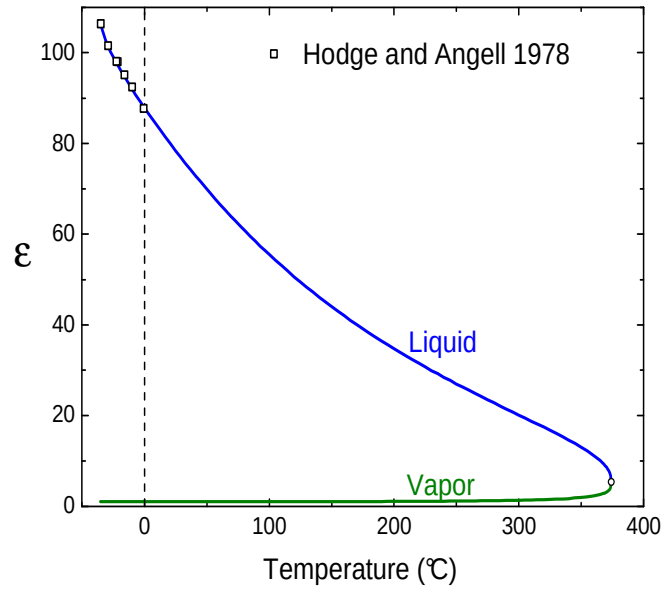

Figure 1. Dielectric constant of water. Solid curves: IAPWS formulation [8]. Symbols: data in supercooled region [9].

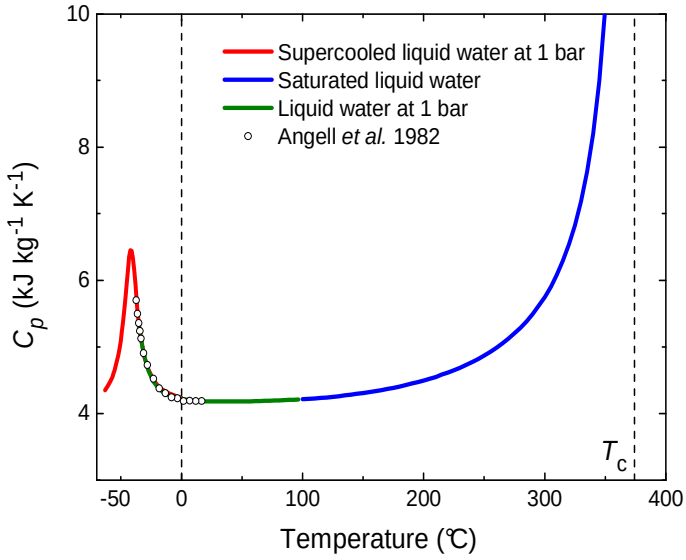

Figure 2. Isobaric heat capacity of liquid water. Solid curve above melting: IAPWS formulation [8]. Symbols: data in supercooled region [7]. Solid curve in supercooled region is calculated from: scaling EOS [10].

capacity that resembles a critical-point-like singularity. In subsequent experiments, the isothermal compressibility [11,12] and thermal expansivity [13,14] were also found to exhibit similar anomalies upon supercooling.

A plausible, thermodynamically consistent, explanation of the global phase behavior of supercooled water was formulated in 1992 by Poole et al.[15]. According to this explanation, there exists a critical point of liquid-liquid coexistence, deep in the supercooled region, which terminates a line of first-order transitions between two liquid phases, namely, a low-density liquid and a high-density liquid. Consequently, the observed anomalies in the heat capacity, compressibility, and thermal expansivity result from the "virtual" divergence of density and entropy fluctuations at this critical point.

In order to coordinate the various experimental findings, we developed a scaled parametric equation of state for the neighborhood of the liquid-liquid critical point in supercooled water [10a]. It was assumed that the liquid-liquid transition in supercooled water does exist and is characterized by a scalar order parameter, and thus belongs to the Ising-model universality class. More recently, we revisited and revised this parametric scaled equation [10b,10c]. Correlating the available experimental data we located the critical point at about 227 K and 28 MPa; the latter is much lower than expected from computer simulations [16]. The suggested location of the second critical point and the liquid-liquid coexistence are shown in Figs. 3 and 4.

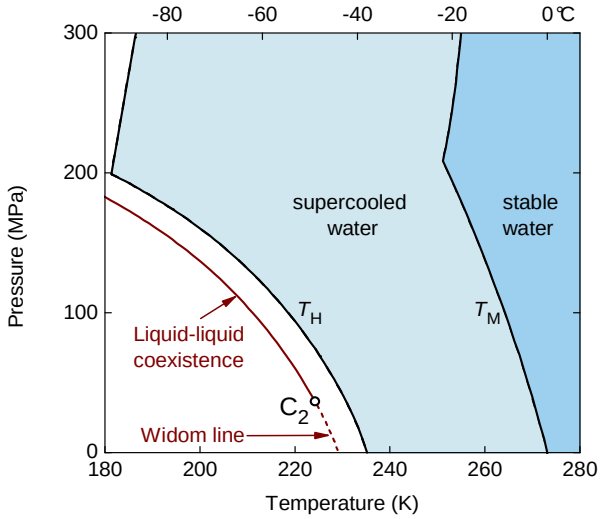

Figure 3. Suggested phase diagram of water with the virtual critical point of liquid-liquid coexistence [10]. C_2 designates the second critical point of water; T_M is the melting line; T_H is the line of spontaneous homogeneous crystallization. The continuation of the liquid-liquid transition line into the homogeneous region is shown by the dashed curve and is known as the Widom line.

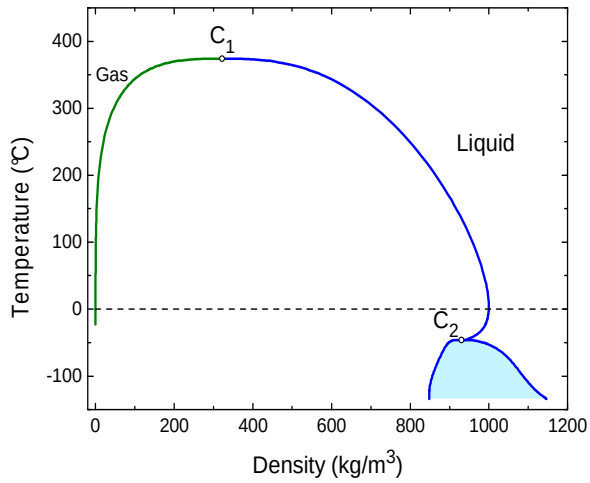

Figure 4. Liquid water polyamorphism: suggested phase diagram of water with the virtual critical point of liquid-liquid coexistence in temperature-density coordinates. C_2 designates the second critical point of water.

In this presentation, I demonstrate the peculiar thermodynamics of the liquid-liquid critical point in supercooled water. It is shown that the liquid-liquid criticality in water represents a special kind of critical behavior in fluids, intermediate between two limiting cases: the lattice gas, commonly used to model gas-liquid transitions, and the "lattice liquid", a weakly-compressible liquid with an entropy-driven phase separation. This peculiar thermodynamics has important practical consequences, in particular, for the behavior of aqueous solutions at low temperatures.

Scaling Fields and Phase Separation in "Lattice Liquid"

Two features make the second critical point in water phenomenologically different from the well-known gas-liquid critical point. The negative slope of the liquid-liquid phase transition line in the *P*-*T* plane means that high-density liquid water is the phase with larger entropy. The relatively large value of this slope at the critical point (about 25 times greater than for the gas-liquid transition at the critical point) indicates the significance of the entropy change relative to the density change, and, correspondingly, the importance of the entropy fluctuations. These features suggest that liquid-liquid phase separation in water is mostly driven by entropy rather than by energy.

The famous lattice-gas model is a symmetric prototype of the liquid-vapor transition in fluids, which, despite its simplicity, reflects the most important features of fluid phase behavior. The lattice-gas model is equivalent to the Ising model for incompressible anisotropic ferromagnets. All fluids belong to the same universality class of criticality as the Ising model. Criticality in the lattice-gas/Ising model is described by two independent scaling fields h_1 and h_2 - designated ordering field and thermal field, respectively - and a third field $h_3(h_1,h_2)$, which is the critical part of the field-dependent thermodynamic potential. The independent scaling fields are thermodynamically conjugate to two scaling densities. The strongly fluctuating scaling density φ_1 (the order parameter) is conjugate to h_1 and the weakly fluctuating scaling density φ_2 is conjugate to h_2. In the lattice-gas model, and, correspondingly, for vapor-liquid critical phenomena, h_1 is associated with the chemical potential μ, while h_2 is the temperature distance ΔT to the critical point. In order to apply the language of Ising criticality to a weakly-compressible single-component liquid that exhibits a liquid-liquid phase transition upon increase of pressure, we considered the following model referred to as "lattice liquid" [10b]. We describe lattice liquid by the Ising scaling fields such that the temperature distance ΔT is taken to be the dominant contribution to h_1, and the pressure distance ΔP is taken to be the dominant contribution to h_2:

$$\begin{aligned} h_1 &= \Delta T + c\Delta P \\ h_2 &= \Delta P \end{aligned}, \qquad (1)$$

where the coefficient c represents the slope of the liquid-liquid coexistence defined as the zero field condition, $h_1 = 0$. Consequently, the major contribution to the order parameter of lattice liquid is the entropy, while the density contribution is proportional to c <<1. Two alternative formulations of the theoretical scaling fields through the physical fields are illustrated in Fig. 5.

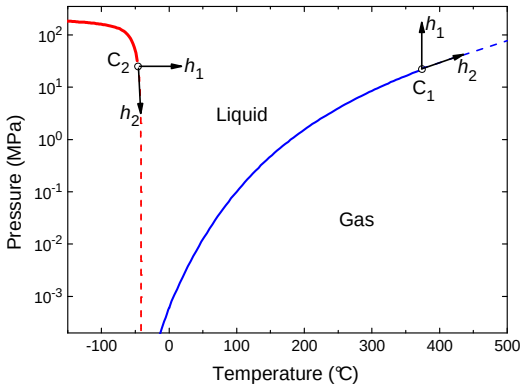

Figure 5. Two alternative formulations for scaling fields in water [10b,10c]. C_1 designates the liquid-vapor critical point and C_2 the liquid-liquid critical point. The Widom line (dashed) corresponds to h_1= 0.

Scaling equation of state cannot be formulated through the scaling fields, h_1 and h_2, in an explicit form. This is why a parametric representation of the critical equation of state [17] appears both elegant and convenient for applications. The simplest form of the scaled parametric equations of state is the so-called "linear model", which represent the scaling fields and the order parameter as functions of the "polar" variables r and θ (Fig. 6):

$$h_1 = ar^{\beta+\gamma}\theta\left(1-\theta^2\right),$$
$$h_2 = r\left(1-b^2\theta^2\right), \qquad (2)$$
$$\varphi_1 = kr^{\beta}\theta,$$

where $\gamma \cong 1.24$ and $\beta \cong 0.325$ are universal critical exponents, the universal coefficient $b^2 = (\gamma - 2\beta)/\gamma(1-\beta) \cong 1.36$, while a and k are system-dependent amplitudes (see more details in refs. [9,17]).

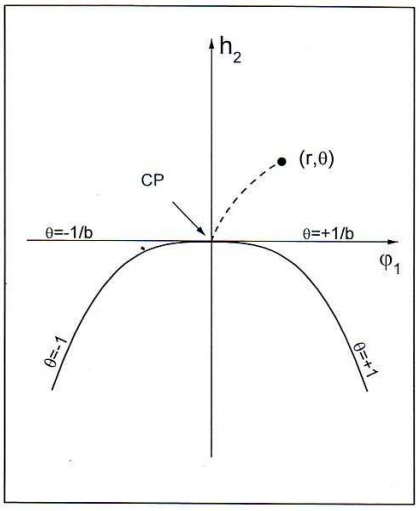

Figure 6. Representation of the thermal ordering field h_2 and the order parameter ϕ_1 through the variables of the parametric "linear model". The ordering field h_1=0 if $\theta = 0$ and $\theta = \pm 1$. Reproduced from ref. [17].

The beauty and simplicity of the linear model is that the singular (critical-fluctuation-induced) behavior of thermodynamic functions is defined by the variable r only, whereas all these functions are analytical with respect to θ.

We have developed a phenomenological mean-field model that clarifies the nature of the order parameter in a polyamorphic single-component liquid and which shares the scaling properties of the lattice liquid. This leads to purely entropy-driven phase separation. Let us assume that the liquid is a "mixture" of two states, A and B, of the same molecular species. For instance, these two states could represent two different arrangements of the hydrogen-bond network in water. We also assume that the individual molecules are identical in both states, leaving aside any concerns regarding the continuity of the fluid phases. The concentration of water molecules involved in either structure, denoted x for state A and 1-x for state B, is controlled by "chemical reaction" equilibrium. Separation into two fluid phases with different equilibrium values of x will occur above the critical pressure P_c. In lowest approximation the solution model assumed to be athermal. While the "regular-solution" model describes the lattice-gas type of the phase diagram, the "athermal-solution" version predicts the liquid-liquid

separation driven only by the non-ideal entropy of mixing. However, unlike an athermal non-ideal binary fluid, the entropy-driven phase separation in a polyamorphic single-component liquid does not happen at any temperature. Contrarily, the critical temperature T_c_ is specified through the critical value of the reaction equilibrium constant.

Real water is undoubtedly more complicated, however, as the following analysis shows, the lattice-liquid model captures the important anomalous features of supercooled water's behavior.

II. Scaling Correlation of Experimental Data

In describing the thermodynamic data for bulk supercooled water we adjust only two critical amplitudes, k and a, the critical pressure, and the backgrounds which are assumed to be regular functions of temperature and pressure. As the first approximation, by using the linear backgrounds, we attributed all the experimentally observed curvatures in the thermodynamic derivatives to the critical-point anomalies [10b]. Moreover, we adopted the location of the liquid-liquid coexistence and its continuation, the Widom line, from an estimate of Mishima [18] and fixed $k=a$. With such a minimalistic approach, we have obtained for ordinary water the following critical parameters of the second critical point: P_c=27.5 MPa and T_c=227.4 K. In particular, we have confirmed our earlier result [10a] that the critical pressure is much lower than that predicted by most of simulations [16]. In the description of bulk heavy water, to minimize the number of adjustable parameters, we adopted all the parameters obtained for ordinary water, including the critical pressure, except for the critical temperature, found to be 235.2 K, and the different linear backgrounds. As a better approximation [10c], we then allowed a small adjustment in the location of the liquid-liquid coexistence without changing the critical pressure and added more analytical terms in the adjustable background of the chemical potential. This approach enables us to nicely describe not only the second derivatives of the free energy but also the density of supercooled water in a broad range of temperatures and pressures. The adjusted value of the critical temperature is 224.2 K. The results of the experimental-data analysis for ordinary water are presented in Figs. 7-10.

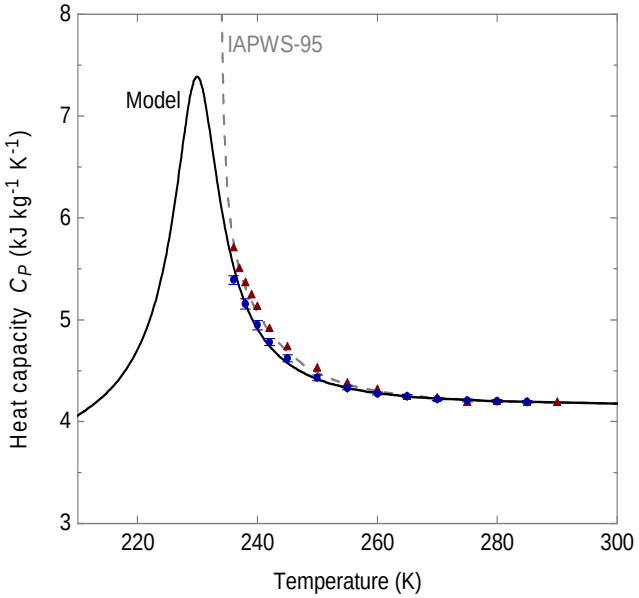

Figure 7. Isobaric heat capacity versus temperature in supercooled water. Solid curve is our model [10c], IAPWS-95 (short dashed) [8]. Symbols represent experimental data of Angell et al. [6] and Archer and Carter [19].

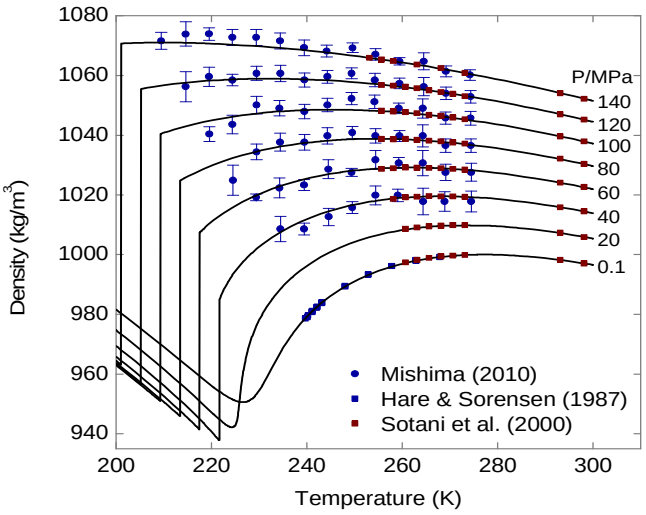

Figure 8. Densities of cold and supercooled water according to our model (curves) [10c]. The symbols represent experimental data of Mishima [18], Sotani et al. [20] and Hare and Sorensen [14]. The symbols for Mishima's densities on different isobars are alternatively open and filled to guide the eye.

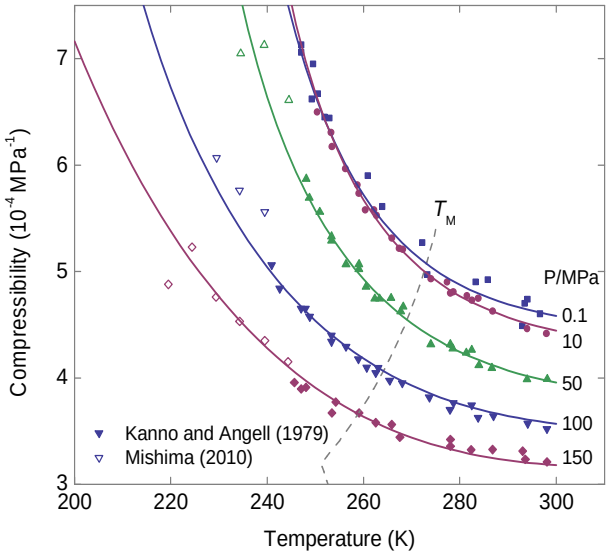

Figure 9. Isothermal compressibility according to our model (curves) [10c]. Symbols represent experimental data of Speedy and Angell [12], Kanno and Angell [13], and Mishima [18]. Solid and open symbols with the same shape correspond to the same pressure.

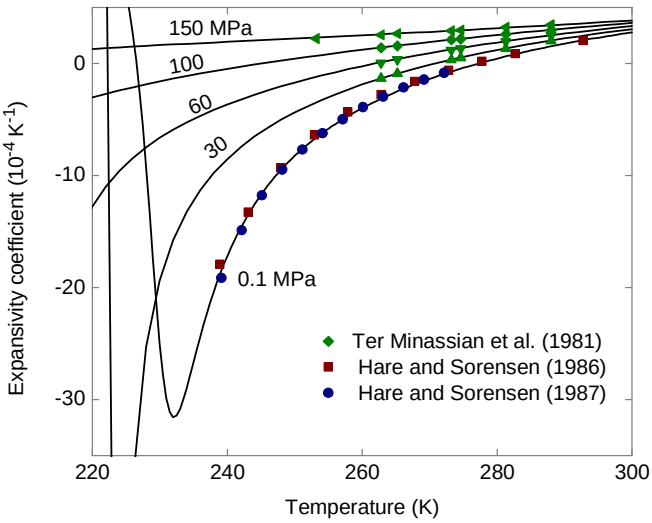

Figure 10. Expansivity coefficient according to our model (solid curves) [10c]. Symbols represent experimental data of Ter Minassian et al. [21] and Hare and Sorensen [13, 14].

III. Confined Supercooled Water

Recent measurements of supercooled water in nanoporous media provide a unique means of testing features of the second critical point hypothesis. In confined water, spontaneous crystallization can be suppressed, allowing for measurements below the bulk homogeneous-nucleation temperature. Much attention has focused on dynamic properties of confined water. Recently, Nagoe et al. [22] have reported maxima in the isobaric heat-capacity of normal and heavy water confined in cylindrical silica MCM-41 nanopores, and investigated the effect of changing the pore diameter. Remarkably, the heat capacity exhibits maxima approximately located along the Widom line predicted for bulk water, where it is not accessible because of spontaneous crystallization. However, the height of the maxima and the shape of the heat capacity in porous media differ significantly from those of bulk water, as seen from Figs. 11a and 11b.

It is known that the behavior of near-critical systems in confined geometries deviates from that seen in bulk as a result of finite-size effects. The theory is known as finite-size scaling [23]. Singular critical-phenomena behavior is observed only when the characteristic size of the system L is much larger than the correlation length of critical fluctuations ξ. In systems, where $L \sim \xi$, finite-size effects may significantly alter the thermodynamic anomalies. In particular, singularities are replaced by L-dependent maxima, the location of these maxima is shifted relative to the bulk critical point, and the anomalous behavior is smeared out over a larger range of temperatures and pressures. Recent measurements of the correlation length in supercooled water suggest that ξ reaches $\sim$1 nm in the supercooled region [24]. The nanopore diameters used by Nagoe et al. vary from $L \sim 1.7$ to ~ 2.4 nm. These sizes are certainly in the range where finite-size effects will be relevant, if not dominant.

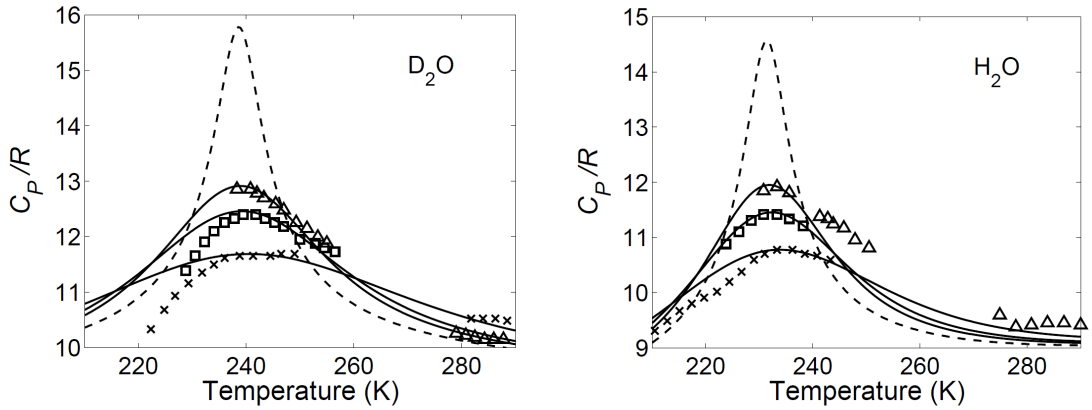

Fig. 11. Heat capacity of supercooled water confined in cylindrical nanopores with different diameters. Symbols are experimental data [23]. Solid curves are predictions of finite-size scaling [10b]. Dashed curve represent bulk water.

It may be dangerous to quantitatively analyze the existing data on water in terms of the conventional theory of finite-size effects, since the cylindrical geometry of the silica MCM-41 nanopores and surface interactions are ignored in the theory. In the absence of an appropriate theory, we have to focus on the qualitative features of finite-size effects. Although the theoretical predictions do not exactly follow the experimental points, they do capture all of the important features qualitatively. In magnetic and fluid systems, finite-size scaling predicts a size-dependent

shift in the temperature and pressure where physical properties exhibit a maximum. Within the experimental errors, all of the curves are interrelated by finite-size scaling through a single characteristic length scale L/ξ.. Finally, the theory predicts that the anomaly is smeared out above the transition temperature, although this effect appears to be more significant for the experimental data than for the predictions of mean-field finite-size scaling. That the smearing is greater for smaller size is best illustrated by the data for heavy water. At the maxima, the 2.4 nm pore heat capacity is greater than the 1.7 nm pore heat capacity but well below the bulk data.

IV. Supercritical-Supercooled: A Novel Supercritical Solvent?

The concept of the second critical point in water raises an intriguing possibility to consider cold water as a novel supercritical solvent. One on the major thermodynamic quantities that control the behavior of supercritical solvents is the so-called Krichevskiĭ parameter [25]. The Krichevskiĭ parameter is defined as

$$K = \lim_{x\to 0}\left(\frac{\partial P}{\partial x}\right)_{T,x} = \frac{dT_c}{dx}\left[\frac{dP_c}{dT_c} - \left(\frac{\partial P}{\partial T}\right)_{V,x}\right], \qquad (3)$$

where x is the mole fraction of solute. Because of the anomalous large value of the derivative $\left(\partial P / \partial T\right)_{V,x}$ for almost incompressible liquid water, the value of the Krichevskiĭ parameter may be very large. Physically, it means that even a very small addition of the solute may significantly affect the properties of cold water and aqueous solutions.

In particular, this feature of cold water may result in the development of new kinds of stable nanoparticles built from small organic molecules. It was recently shown [26] that micro doping of propylene oxide into aqueous solutions of tert-butanol, produce

100 nm particles. Figure 12 shows the light-scattering intensity auto-correlation function of cold-filtered TBA aqueous solution after the addition of 7×10^{-5} mole fraction PO at 8.5 °C. After the addition of PO, the mesoscale particles, previously removed by cold filtration, re-emerge, as indicated by a sharp increase in the light-scattering intensity and the appearance of the slow diffusive relaxation mode in the correlation function. This sample has been monitored for about 3 months, and no significant change of the nanoparticle size is observed.

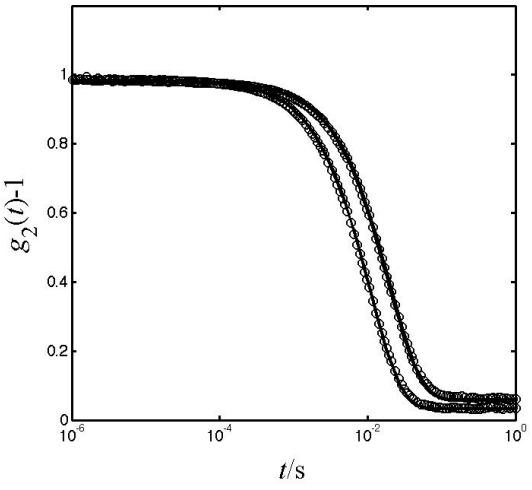

Figure 12. Light-scattering **i**ntensity auto-correlation functions for 0.073 mol fr tert-butanol cold-filtered aqueous solution, doped with a micro mole amount of propylene oxide, at the scattering angle $\theta = 60^{\circ}$ and $T = 8.5\,^{\circ}$C. Right-side curve is slow cooling (5 K/hr). Left-side curve is fast cooling (3 K/min)

V. Conclusion

In this presentation, it is assumed that the liquid-liquid critical point in water does exist. Although I consider this scenario as most plausible, other interpretations of the anomalies in supercooled water still worth attention. Some experiments in confined water [27] may be interpreted as a second-order phase transition line or a weakly first-order transition line, replacing what is commonly believed to be the Widom line. Such an interpretation would be more radical than any of the scenarios suggested for supercooled water thus far because it requires the existence of a vector-like order parameter similar to that in the super-fluid liquid helium. Most recently, the discussion on the nature of the anomalies observed in supercooled water has received an additional impetus after Limmer and Chandler reported new simulation results [28] for two atomistic models of water. They found only a single liquid state in the supercooled region and excluded the possibility of the liquid-critical point for the models studied. It would be important to compare the anomalies predicted by the models with those exhibited by real water. The final conclusion on the existence of the liquid–liquid critical point in water should be based on the ability to explain and quantitatively describe the experimental data. The information provided in this presentation shows that a critical-point parametric equation of state describes the available thermodynamic data on supercritical water within experimental accuracy, thus establishing a benchmark for any further developments in this research area.

Acknowledgments

I acknowledge collaboration with C. B. Bertrand, D. A. Fuentevilla, V. Holten, J. Kalova, D. Subramanian, and J. V. Sengers. The research is supported by the Division of Chemistry of the National Science Foundation (Grant No. CHE-1012052).

References

1. Voronel, A. V., JETP Lett. 1971, **14**, 174-177.
2. Voronel, A. V. In: “Phase Transitions and Critical Phenomena”; Domb, C.; Green, M. S., Eds.; Academic Press: London, 1976, Vol. 5B, pp. 343-391.
3. Anisimov, M. A.; Voronel, A. V.; Zaugol'nikova, N. S.; Ovodov, G. I. JETP Lett. 1972, **15**, 317-319.
4. Angell, C. A.; Shuppert, J.; Tucker, J. C. J. Phys. Chem. 1973, **77**, 3092-3099.
5. Rasmussen, D. H.; MacKenzie, A. P. J. Chem. Phys. 1973, **59**, 5003-5013.
6. Oguni, M.; Angell, C. A. J., Chem. Phys. 1980, **73**, 1948-1954.
7. Angell, C. A.; Oguni, M.; Sichina, W. J., J. Phys. Chem. 1982, **86**, 998-1002
8. Revised Release on the IAPWS Formulation 1995 for the Thermodynamic Properties of Ordinary Water Substance for General and Scientific Use, IAPWS (2009).
9. Hodge, I. M., Angel C. A., J. Chem. Phys. 1978, **68**, 1363-1368.
10. (a) Fuentevilla, D. A.; Anisimov, M. A., Phys. Rev. Lett. 2006, **97**, 195702/1-195702/4; ibid. 2007, **98**, 149904/1, (b) Bertrand, C. E., Anisimov, M. A, J. Phys. Chem. B 2011, in press (doi: 10.1021/jp204011z). (c) Bertrand C. E., Holten, V., Anisimov, M. A., Sengers, J. V., “Thermodynamic modeling of supercooled water”, Technical Report for the International Association for the Properties of Water and Steam (IAPWS), September 2011.

11. Kanno, H.; Angell, C. A., J. Chem. Phys. 1979, **70**, 4008-4016.
12. Speedy, R. J.; Angell, C. A., J. Chem. Phys. 1976, **65**, 851-858.
13. Hare, D. E.; Sorensen, C. M., J. Chem. Phys. 1986, **84**, 5085-5089.
14. Hare, D. E.; Sorensen, C. M., J. Chem. Phys. 1987, **87**, 4840-4845.
15. Poole, P. H.; Sciortino, F.; Essmann, U.; Stanley, H. E., Nature 1992, **360**, 324-328.
16. Sastry, S.; Sciortino, F.; Stanley, H. E., J. Chem. Phys. 1993, **98**, 9863-9872. Poole, P. H.; Sciortino, F.; Essmann, U.; Stanley, H. E., Phys. Rev. E 1993, **48**, 3799-3817. Poole, P. H.; Essmann, U.; Sciortino, F.; Stanley, H. E., Phys. Rev. E 1993, **48**, 4605-4610. Stanley, H. E.; Angell, C. A.; Essmann, U.; Hemmati, M.; Poole, P. H.; Sciortino, F., Physica A 1994, **205**, 122-139.
17. Behnejad, H.; Sengers, J. V.; Anisimov, M. A. In: "Applied Thermodynamics of Fluids"; Goodwin, A.; Sengers, J. V.; and Peters, C. J., Eds.; IUPAC, RSC Publishing: Cambridge, 2010, pp. 321-366.
18. Mishima, O. J., Chem. Phys. 2010, **133**, 144503/1-144503/6.
19. Archer, D. G.; Carter, R. W., J. Phys. Chem. B 2000, **104**, 8563-8584.
20. Sotani, T., Arabas, J., Kubota, H., Kijima, M., High Temp. High Pressures 2000, **32**, 433.
21. Ter Minassian, L,. Pruzan, P., Soulard, A., J. Chem. Phys. 1981, **75**, 3064.
22. Nagoe, A.; Kanke, Y.; Oguni, M.; Namba, S. J., Phys. Chem. B, 2010,**114**, 13940-13943.
23. Fisher, M. E.; Barber, M. N., Phys. Rev. Lett. 1972, 28, 1516-1519. Rudnick, J.; Guo, H.; Jasnow, D. J., Stat. Phys. 1985, **41**, 353-373.
24. Huang, C.; Weiss, T. M.; Nordlund, D.; Wikfeldt, K. T.; Pettersson, L. G. M.; Nilsson, A., J. Chem. Phys 2010, **133**, 134504/1-134504/5.
25. Anisimov, M. A., Sengers, J. V., Levelt Sengers, J. M. H., In "The Physical Properties of Aqueous Systems at Elevated Temperatures and pressures: Water, Steam and Hydrothermal Solutions", D. A. Palmer, R. Fernandez-Prini, and A. H. Harvey, eds., pp. 29-72, Academic Press, 2004.
26. Subramanian, D., Anisimov, M. A., J. Phys. Chem. B 2011, **115**, 9179-9183.
27. Chang, S.; Chen, S.-H., arXiv:1005.5387v2 [cond-mat.soft], 2010.
28. Limmer, D.T., Chandler, D., arXiv:1107.0337v1 [cond-mat.stat-mech] (2011).